Excitatory amino acid transporter 1 supports adult hippocampal neural stem cell self-renewal.

Joshua D. Rieskamp[1], Ileanexis Rosado-Burgos[1], Jacob E. Christofi[1], Eliza Ansar[1], Dalia Einstein[1], Ashley E. Walters[1], Valentina Valentini[1,4], John P. Bruno[1,2], Elizabeth D. Kirby[1,2,3*]

[1]Department of Psychology, [2]Department of Neuroscience, [3]Chronic Brain Injury Program, The Ohio State University, USA, [4]Department of Biomedical Sciences, University of Cagliari, Italy

*Corresponding author email: kirby.224@osu.edu

Summary:

Within the adult mammalian dentate gyrus (DG) of the hippocampus, glutamate stimulates neural stem cell (NSC) self-renewing proliferation, providing a link between adult neurogenesis and local circuit activity. Here, we show that glutamate-induced self-renewal of adult DG NSCs requires glutamate transport via excitatory amino acid transporter 1 (EAAT1) to stimulate lipogenesis. Loss of EAAT1 prevented glutamate-induced self-renewing proliferation of NSCs in vitro and in vivo, with little role evident for canonical glutamate receptors. Transcriptomics and further pathway manipulation revealed that glutamate simulation of NSCs relied on EAAT1 transport-stimulated lipogenesis, likely secondary to intracellular Ca^{2+} release and glutamate metabolism. Our findings demonstrate a critical, direct role for EAAT1 in stimulating NSCs to support neurogenesis in adulthood, thereby providing insights into a non-canonical mechanism by which NSCs sense and respond their niche.

Keywords: neural stem cell, adult neurogenesis, glutamate, excitatory amino acid transporter, hippocampus

Introduction

The dentate gyrus of the hippocampus (DG) is one of a few, isolated brain regions that can support resident neural stem cells (NSCs) that generate new neurons in adult mammals. Adult hippocampal NSCs are distinct from developmental counterparts[1–3], and their persistence through adulthood is conserved across most land-born mammals, likely including primates[4–7] (but see:[8,9]). The excitatory neurotransmitter glutamate is a potent stimulator of NSC proliferation in the adult DG, a link which suggests a mechanism for tethering adult neurogenesis to circuit activity, as well as a potential mechanism for regeneration in excitotoxic conditions[10,11].

Recent work shows that glutamate promotes asymmetric, self-renewing NSC divisions[12–14]. However, the molecular mediator by which glutamate stimulates NSCs is unclear. Early studies found that NDMA receptor antagonists actually increase NSC proliferation, rather than decrease it[15–18]. More recently, it was shown that triple transgenic knockout of AMPA, NMDA and metabotropic glutamate receptors in NSCs had no effect on their proliferation[14]. Together, previous work suggests that the NSC response to glutamate is unlikely to rely on simple receptor stimulation.

A major component of glutamate regulation in the adult mammalian brain is the family of excitatory amino acid transporters (EAATs). EAATs are transmembrane transporters that shuttle glutamate from the extracellular to intracellular environment via ion-coupled transport. Robust EAAT expression, in particular EAAT1, is a widely-used marker of adult NSC phenotype[19,20] and

in vivo transport-associated currents suggest these transporters are present and active in the adult DG NSC membrane[21–23]. The functional role of EAATs in NSC regulation has received little attention to date. To better understand how adult NSCs interact with the glutamatergic environment of the adult mammalian DG, we set out to uncover the functional role of EAATs in these cells.

Results

High expression of EAAT1, but not other EAATs, is widespread in NSCs and declines rapidly with differentiation

The EAAT family of glutamate transporters has 5 primary members, EAAT1, 2, 3 ,4 and 5 (gene names Slc1a3, Slc1a2, Slc1a1, Slc1a6, Slc1a7). Adult DG NSCs have been reported to express both EAAT1 and EAAT2[21]. Using single cell RNAseq (scRNAseq) data from Shin et al.[24], we confirmed that adult DG NSCs express EAAT1 (Slc1a3) and EAAT2 (Slc1a2) but not the remaining 3 EAATs (Fig S1A,B). EAAT2 expression was ~5.35x lower than EAAT1. To verify the extent of EAAT1 and 2 expression throughout NSCs in vivo, we used immunolabeling in adult EAAT1dsRed and EAAT2GFP transcriptional reporter mice[21] (Fig 1A,B, S1C). ~53% of

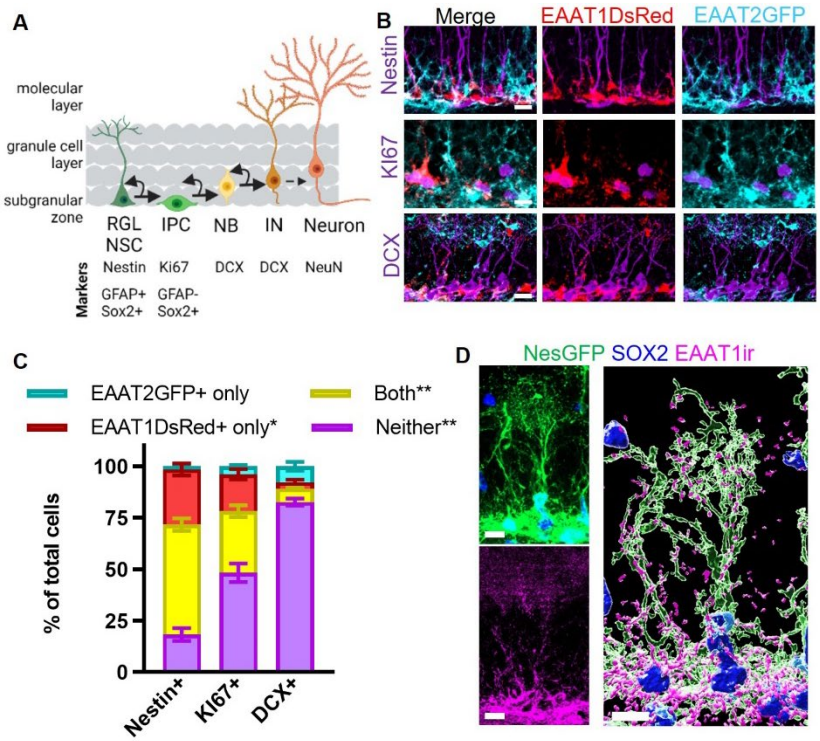

Figure 1: NSC express EAAT1 and to a lesser extent EAAT2

A) Cells in the neurogenic cascade along with immunophenotypical markers used to identify radial glial like NSCs (RGL NSC), intermediate progenitor cells (IPCs), neuroblasts (NB), immature neurons (IN) and mature neurons.

B) Immunolabeling for Nestin, Ki67 and DCX in DG from EAAT1DsRed+EAAT2GFP+ adult mice.

C) Proportion of cells expressing EAAT1DsRed+EAAT2GFP+ in adult DG. *p<0.05,**p<0.01 Tukey's posthoc test. Mean ± SEM of N = 4-5 mice.

D) EAAT1 immunolabeling in NestinGFP+ NSC, with Sox2+ nucleus. Merged z-stack on left, 3D reconstruction of z-stack on right.

All scales = 10 µm.

Nestin+ radial glia-like NSCs were positive for both EAAT1dsRed and EAAT2GFP, with another ~27% positive for EAAT1dsRed alone (Fig 1B,C, S1D). Less than 2% of Nestin+ NSCs were positive for EAAT2GFP alone, leaving ~18% of Nestin+ NSCs negative for either transporter. Ki67+ proliferative cells in the subgranular zone, which are primarily composed of intermediate progenitor cells (IPCs), and doublecortin (DCX+) neuroblasts and immature neurons each showed progressively smaller proportions of cells expressing EAATs. Using 3D image reconstruction of EAAT1 immunolabeling in adult NestinGFP mice[25], as well as nestin immunolabeling in EAAT1dsRed mice, we also showed EAAT1 protein putatively co-localizing throughout the NSC cell soma and in the bushy terminals in the molecular layer (Fig 1D, S1E). Together, these data suggest that EAAT1, and to a lesser extent EAAT2, are expressed throughout adult DG NSCs, with rapid downregulation upon differentiation.

Glutamate stimulates adult NSCs via EAAT-mediated transport.

To begin investigating the role of EAATs in NSCs, we used cultured NSCs derived from adult male and female DG[26]. These cultures are composed primarily of quiescent and cycling NSCs when maintained in standard conditions[27]. Using our published bulk RNAseq and liquid chromatography tandem mass spectrometry data from these cells[27], we first confirmed that cultured NSC expression of glutamate transporter and receptor genes was similar to that of in vivo NSCs, with EAAT1 being most abundant, followed by EAAT2, then lower but detectable expression levels of AMPA receptor subunits and metabotropic glutamate receptor transcripts (Fig S2A-C). We also confirmed that glutamate stimulated NSC proliferation, as revealed by incorporation of the thymidine analog ethynyl deoxyurdine (EdU) (Fig 2A,D).

To determine the role of glutamate receptors versus transporters in NSC proliferation, we treated NSCs with several pharmacologic inhibitors. Treatment with a cocktail of inhibitors to block AMPA, NMDA and mGluR5 (NBQX, D-AP5, and ACDPP, referred to together as αGlut R) had no effect on basal NSC proliferation nor their response to glutamate (Fig 2B,E). The panEAAT inhibitor TFB-TBOA (αpanEAAT), in contrast, blocked glutamate-induced proliferation and did so whether glutamate receptors were inhibited or not. Aspartate, an alternate transport substrate for both EAAT1 and 2, also stimulated NSC proliferation in an EAAT-dependent, receptor-independent manner (Fig 2C, S2D). To further explore the role of glutamate receptors in NSC proliferation, we treated NSCs with glutamate receptor agonists: AMPA, KA, NMDA and CHPG (mGluR5 agonist). None of the agonists increased proliferation (Fig 2F, S2E). NMDA slightly decreased proliferation. CHPG (mGluR5) agonist caused massive cell death at its higher dose and had no effect at its lower dose. These findings suggest, unexpectedly, that EAAT transporter activity alone mediates glutamate-induced NSC proliferation with no, or possibly a countering, contribution of glutamate receptors.

Glutamate stimulation of adult NSCs relies on EAAT1 not EAAT2.

To determine which EAATs might be active in NSCs, we measured glutamate clearance from NSC cultures using ultra-high performance liquid chromatography with electrochemical detection (uHPLC-ECD) of conditioned media. Within 20 minutes, NSCs cleared 82% of a 5 μM glutamate pulse from the media (Fig S2F). Treatment with the selective EAAT1 inhibitor (UCPH101, αEAAT1) or a combination of αEAAT1 and the selective EAAT2 inhibitor (WAY213613, αEAAT2) completely prevented glutamate clearance compared to vehicle treated controls (Fig 2G). αEAAT2 alone had no effect on clearance compared to vehicle treated controls. To confirm activity of the αEAAT2 drug, we replicated the experiment with a higher

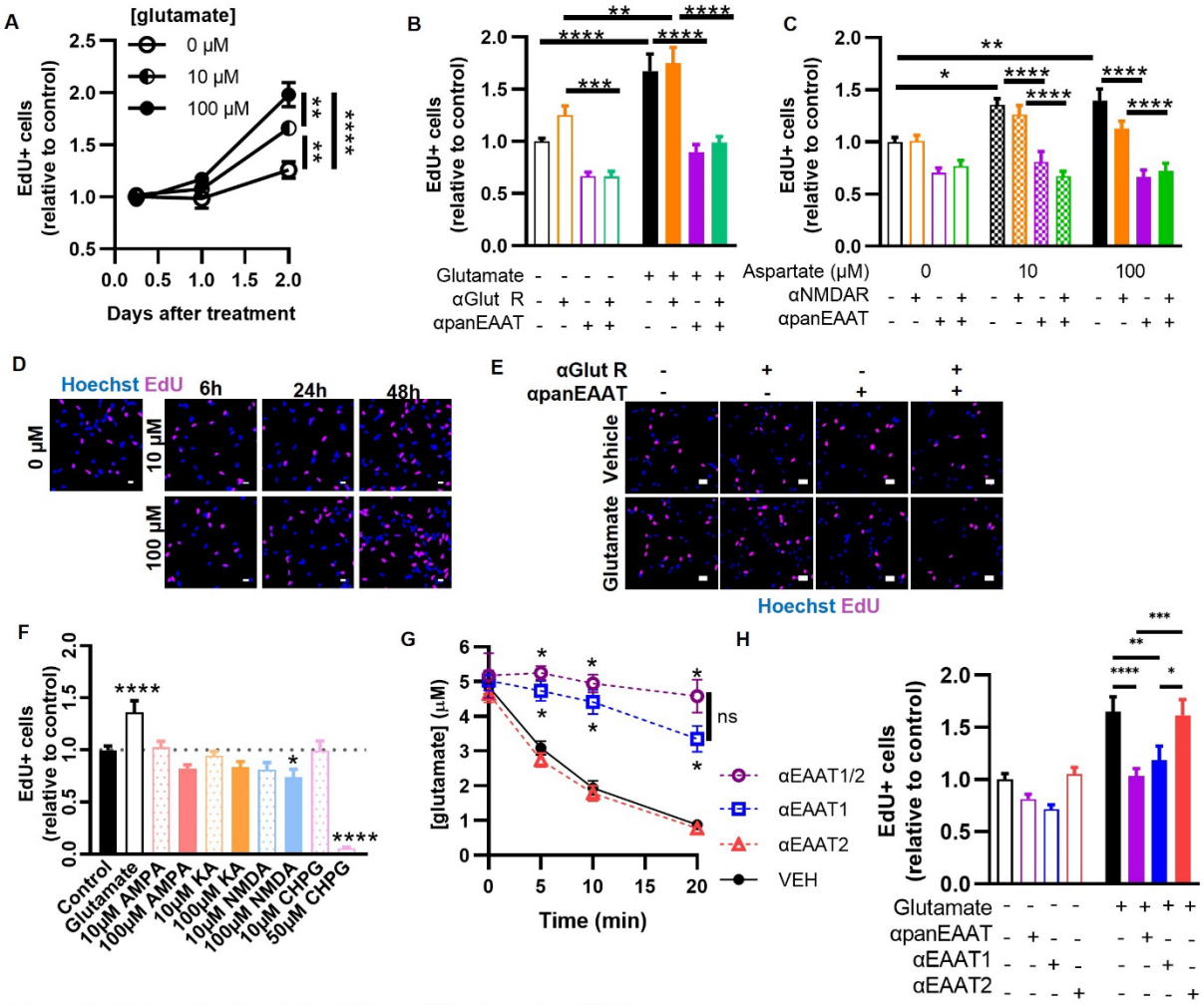

Figure 2: Glutamate stimulates NSC proliferation via EAAT1.
A-C) EdU+ cell counts after treatment with: glutamate, inhibitors of glutamate receptors (αGlutR, NBQX, D-AP5, and ACDPP), inhibitor of EAATs (αpanEAAT, TFB-TBOA), aspartate, inhibitor of NMDA receptor (αNMDAR). Mean ± SEM of N = 2-5 replicates/experiment, 3-4 independent experiments.
D-E) Representative images of EdU+ labeling in cultured NSCs after glutamate treatment +/- receptor and transporter inhibitors, with Hoechst to label nuclei. Scale = 20 μm.
F) EdU+ cell counts after treatment with glutamatergic agonists. Mean ± SEM of N = 6-12 replicates/experiment, 4 independent experiments.
G) Glutamate in NSC conditioned media as measured by uHPLC after a 5 μM pulse with pretreatment with inhibitors of EAAT1 (UCPH102), EAAT2 (WAY213613) or their combination (EAAT1/2). Mean ± SEM of N = 3 independent experiments.
H) EdU+ cell counts after treatment with glutamate +/- inhibitors of EAAT1 (UCPH102), EAAT2 (WAY213613), or panEAAT (TFB-TBOA). Mean ± SEM of N = 5 replicates/experiment, 3 independent experiments.
All EdU+ counts expressed relative to 0 μM glutamate/vehicle within experiment. *,**,***,****p<0.05, <0.01, 0.001, 0.0001 posthoc comparisons.

dose that also inhibits EAAT1. Higher dose αEAAT2 partially prevented glutamate clearance, suggesting that the compound is active but only shows effects at doses that inhibit EAAT1 (Fig S2G). Similar results were found with an alternative EAAT2 inhibitor (DHK) (Fig S2H). Taken together, these results demonstrate functional glutamate clearance by NSCs and implicate EAAT1 as the dominant transporter.

We next treated cultured NSCs with αEAAT1, αEAAT2 or αpanEAAT and measured proliferation. Both EAAT1 and panEAAT inhibition each prevented glutamate-induced NSC

proliferation while EAAT2 inhibition alone had no effect (Fig 2H, S2I). Throughout these experiments, cells in all groups appeared healthy and showed no observable signs of apoptosis (fragmented nuclei, loss of plate adhesion). We also confirmed that neither αpanEAAT nor αEAAT1 led to signs of cell death using a Sapphire700 IR dye assay (Fig S2J). Together, these data suggest that glutamate stimulates NSC proliferation directly via EAAT1 activity.

EAAT1 knockdown causes cell-autonomous loss of NSC self-renewal in vivo

To examine the role of EAAT1 in DG NSCs in vivo, we used CRISPR interference (CRISPRi), a transcriptional interference strategy based on the CRISPR/cas9 system. In CRISPRi, a catalytically dead Cas9 protein (dCas9) fused to a Kruppel associated box (KRAB) domain represses transcription of a gene targeted by a highly specific single guide (sg)RNA. We designed a U6→sgRNA against EAAT1 (EAAT1 KD) (and a non-target sgRNA (NT)) then inserted it into a lentiviral CRISPRi backbone[28] with dCas9-KRAB-T2A-GFP (Fig 3A). Cultured NSCs infected with the EAAT1 KD CRISPRi vector showed a 53.1% loss of EAAT1 immunoreactivity and significant suppression of proliferation compared to NT infected cells (Fig S3A-C). We stereotaxically infused the EAAT1 KD and NT CRISPRi lentiviral vectors in the DG of adult mice. 1 week later, no loss of EAAT1 protein was detected (Fig S3E,F). 3 weeks later, a 40.6% knockdown of EAAT1 immunoreactivity was detected in EAAT1 KD compared to NT treated controls (Fig S3G,H). We therefore next assessed the effect of EAAT1 loss on the neurogenic cascade at this 3 week timepoint.

In this paradigm, EAAT1 knockdown could alter NSCs via receptor-independent, cell-autonomous loss of glutamate transport, as our in vitro data suggests, or through increased glutamate stimulation of receptors due to extracellular glutamate buildup, or through a combination of the two. To investigate the cell autonomous effect, we compared dCas9-KRAB-GFP+ NSCs (hereafter GFP+ NSCs) to neighboring GFP- NSCs. While changes in ambient glutamate would affect both GFP+ and GFP- NSCs, only the GFP+ NSCs would be lacking cell autonomous glutamate transport. At 3 weeks after viral infusion, EAAT1 KD mice had 53.9% fewer GFP+GFAP+SOX2+ radial glia-like NSCs compared to NT treated controls (Fig 3B,C). In contrast, the neighboring GFP- NSCs in these mice showed no effect of EAAT1 KD. The number of proliferating (EdU+) GFP+GFAP+ radial glia-like NSCs showed the same pattern, with a 63.5% decrease in density of proliferating GFP+ NSCs with EAAT1 KD but no effect on neighboring GFP- proliferating NSCs compared to NT control mice (Fig 3D,E). No differences were found between NT and EAAT1 KD mice in GFP+ or GFP- GFAP-SOX2+ IPC density nor in density of DCX+ neuroblasts/immature neurons that were BrdU-labeled 2 weeks before perfusion (Fig 3F,G, S3I). These findings suggest that loss of EAAT1 causes a cell-autonomous loss of radial glia-like NSC self-renewal.

To determine whether the loss of NSCs observed at 3 weeks after knockdown would result in loss of adult neurogenesis at longer timepoints, we perfused mice 2 months after NT or EAAT1 KD CRISPRi lentiviral infusion (Fig 3H). EAAT1 KD mice showed a 63.0% loss of GFP+ radial glia-like NSCs with no effect on GFP- NSCs compared to NT control mice (Fig 3I,K). Similar to NSCs, GFP+ IPC density was 54.3% lower in EAAT1 KD mice compared to NT control mice, while density of GFP- IPCs did not differ between EAAT1 KD and NT mice (Fig 3J). EAAT1 KD mice also showed a 73.6% reduction in number of GFP+NeuN+ newborn neurons labeled with BrdU 1 month before perfusion and no effect on GFP-NeuN+BrdU+ cells (Fig 3L,M, S3J). These data suggest that loss of EAAT1 results in loss of adult neurogenesis that is restricted to the progeny of NSCs that lost EAAT1 and does not extend to neighboring NSCs and their progeny.

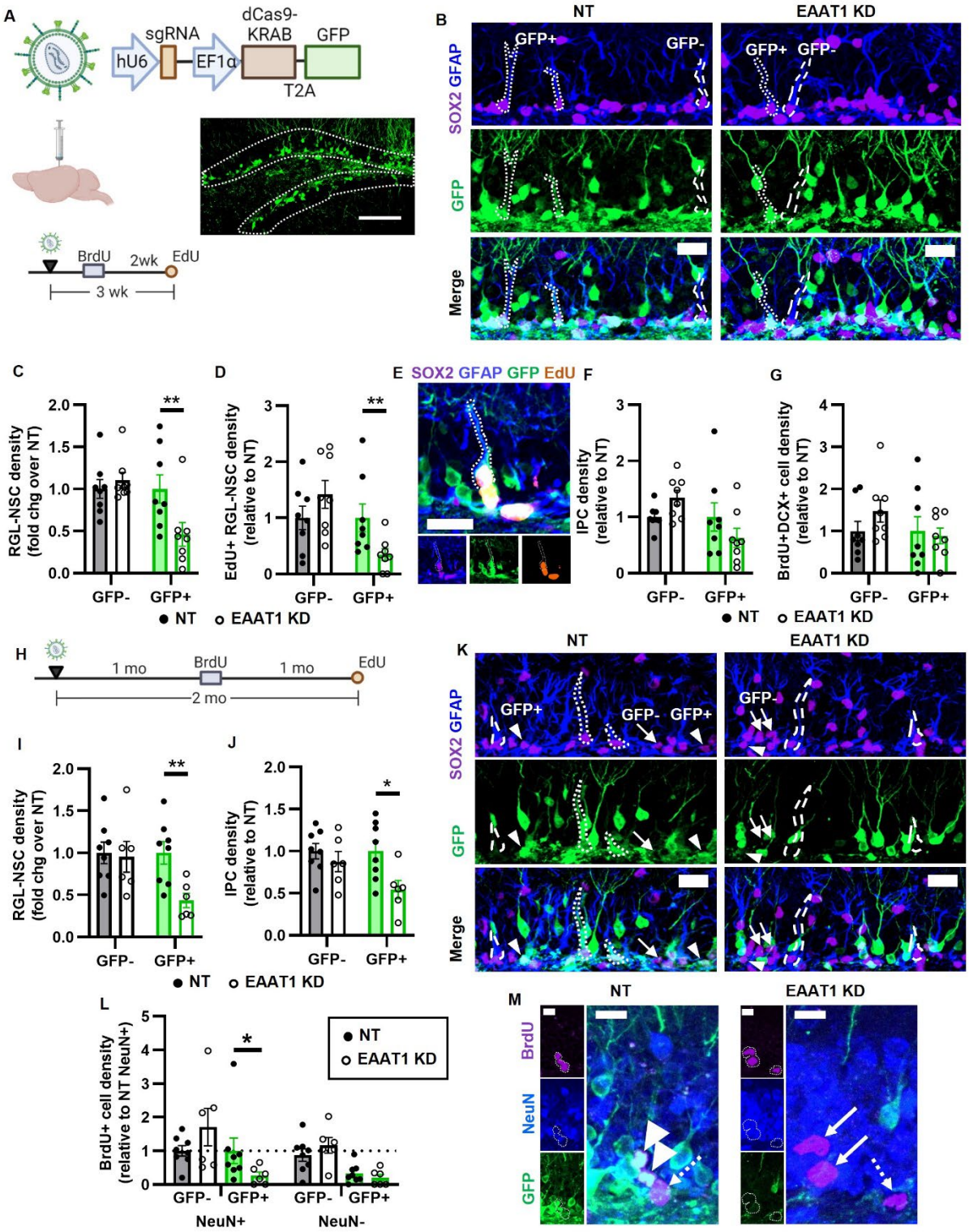

Figure 3: EAAT1 knockdown causes cell-autonomous loss of NSC self-renewal

A) CRISPRi lentiviral vector design and timeline. Inset image show representative GFP+ labeling in DG at 3 weeks after infusion. Scale = 100 µm.

B,K) Representative images of GFAP, SOX2, GFP immunolabeling for quantification of NSCs and IPCs 3 weeks (B) and 2 mo (K) after infusion. GFP+ and GFP- NSCs are outlined in C. IPCs are also shown by arrows (GFP-) or arrowheads (GFP+) in K. Scale = 20 µm. (legend continued on next page)

Figure 3 (cont): EAAT1 knockdown causes cell-autonomous loss of NSC self-renewal
C-D) Density of GFP+ and GFP- GFAP+SOX2+ total (C) and EdU+ (D) radial glia-like NSCs in NT and EAAT1 KD mice 3 weeks after infusion.
E) Representative image of an EdU+GFP+GFAP+SOX2+ radial glia-like NSC 3 weeks after infusion. Scale = 10 µm.
F,G) Density of GFP+ and GFP- GFAP-SOX2+ IPCs (F) and DCX+BrdU+ newborn neuroblasts/immature neurons (G) in NT and EAAT1 KD mice 3 weeks after infusion.
H) Timeline for panels I-M
I,J) Density of GFP+ and GFP- GFAP+SOX2+ radial glia-like NSCs (I) and GFAP-SOX2+ IPCs (J) in NT and EAAT1 KD mice 2 months after infusion.
K) Density of GFP+ and GFP- BrdU+ cells (NeuN+ and NeuN-) in NT and EAAT1 KD mice 2 months after infusion.
L) Representative images of BrdU+ cells.
All densities relative to NT control within GFP type. Arrowhead = BrdU+NeuN+GFO+, Arrow = NeuN+BrdU+, Dashed arrow = BrdU+. Scale = 10 µm.
C,D,F,G: Mean ± SEM of N = 8 individual mice (points shown). *,**p<0.05, 0.01 Sidak's multiple comparisons within GFP label type.
I,J,L: Mean ± SEM of N = 6-8 individual mice (points shown). *,**p<0.05, 0.01 Sidak's multiple comparisons within GFP label type

EAAT-dependent stimulation of fatty acid synthetase is essential for glutamate-induced NSC proliferation.

To gain insight into the molecular mediators of EAAT-dependent stimulation of NSC self-renewal, we performed bulk RNAseq on RNA from cultured NSCs treated with glutamate and/or panEAAT inhibitor (Fig S4A). In the absence of αpanEAAT, glutamate treatment caused significant upregulation of 106 transcripts and significant downregulation of 49 transcripts (Table S1). In contrast, in the presence of αpanEAAT, glutamate treatment yielded no upregulated transcripts and only 1 downregulated transcript. These data suggest robust NSC transcriptional response to glutamate that is prevented by EAAT inhibition.

To understand the functional significance of genes regulated by glutamate transport, we focused on GO biological process analysis of genes upregulated by glutamate that were also downregulated by αpanEAAT (Table S2). We found 22 overlapping GO terms which centered mostly on metabolic processes related to lipid, amino acid, and protein synthesis (Fig 4A). Particularly notable among the cellular processes implicated in EAAT-dependent regulation of NSC gene expression was lipid biosynthetic process. Lipogenesis is essential for NSC self-renewal, with a particularly critical role for fatty acid synthetase (FASN)[29–31]. In our RNAseq data, glutamate induced upregulation of Fasn, an effect that EAAT inhibition blocked (Table S1,S3). Independent replication using qPCR confirmed that glutamate stimulated Fasn expression in an EAAT-dependent manner (Fig 4B). FASN inhibition with the inhibitor orlistat also prevented glutamate-induced NSC proliferation (Fig 4C, S4B). These findings suggest that glutamate transport by EAAT promotes NSC proliferation via stimulation of FASN.

Glutamate stimulation of NSCs requires both transport-associated Ca^{2+} signaling and glutamate metabolism.

We next sought to determine the upstream signals that could mediate NSC proliferation in response to glutamate transport. In Bergmann and Müller glia, glutamate transport can act as an intracellular signaling event by triggering a Ca^{2+}-dependent signaling cascade culminating in phosphorylation and activation of mTOR[32,33], which itself promotes de novo lipogenesis and proliferation in adult stem cells, including NSCs[34,35]. Similar to these specialized glial cells, we found that glutamate induced mTOR phosphorylation in adult DG NSCs and that effect was blocked by EAAT inhibition (Fig 4D, S4C). In Bergmann and Müller glia, the Ca^{2+} signal that

drives mTOR phosphorylation derives from the co-transport of $3Na^+$ with glutamate via EAATs, which causes reversal of the Na^+-Ca^{2+} transporter, NCX, to export Na^+ and import Ca^{2+}. In adult NSCs, though, treatment with either of 2 NCX inhibitors, SEA0400 or YM 244769, had no effect on basal or glutamate-stimulated NSC proliferation (Fig S4D-F). These data suggest that Ca^{2+} influx via NCX reversal is not a likely mediator of EAAT-dependent stimulation of proliferation.

We next examined an alternate source of Ca^{2+} release: the Ca^{2+} stores of the endoplasmic reticulum (ER). Glutamate transport via EAATs is accompanied by net depolarization due to co-transport with $3Na^+$ and $1H^+$ (plus export of $1K^+$). Cellular depolarization is a potent stimulator of

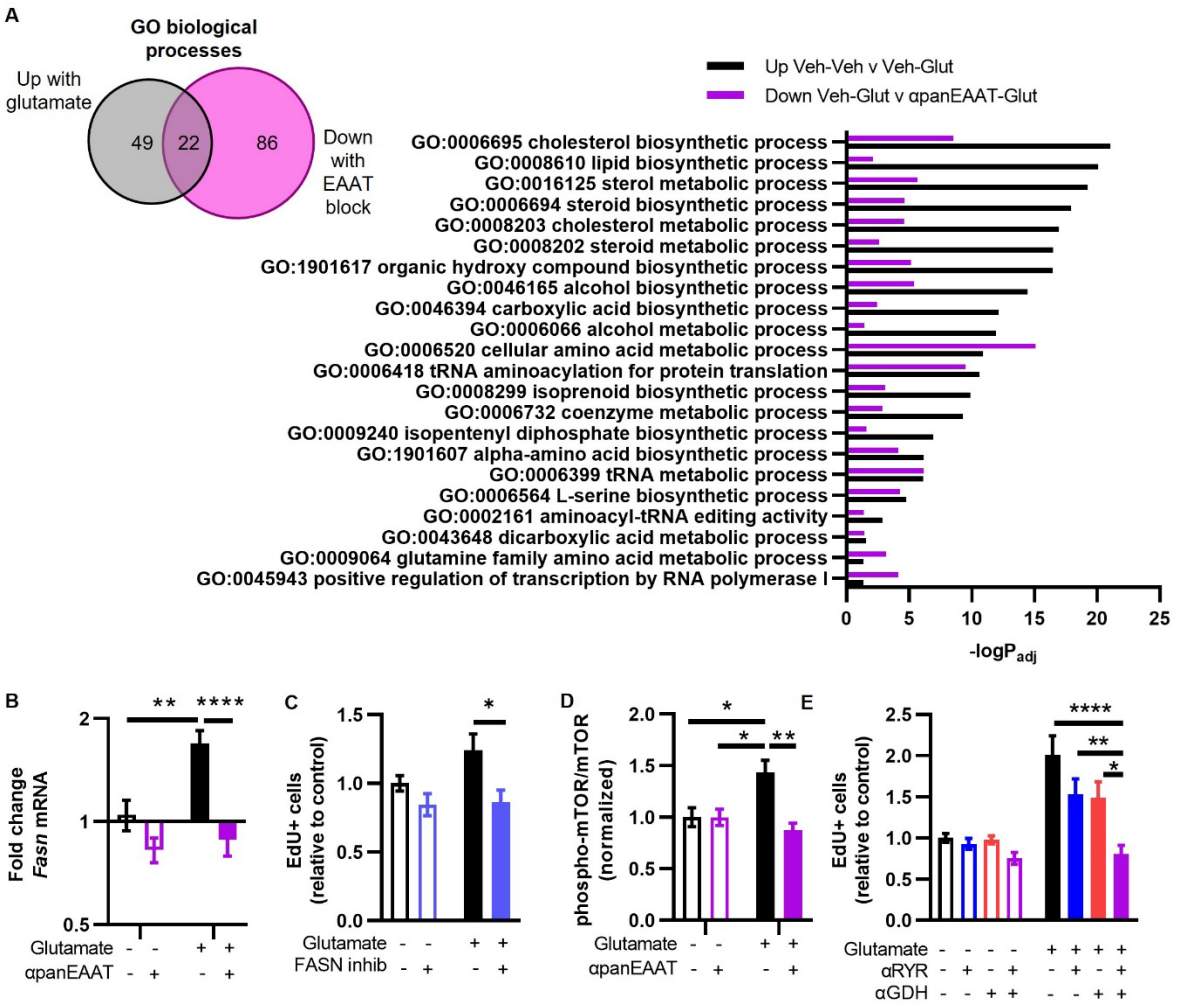

Figure 4: Glutamate stimulates NSC self-renewal via transport-stimulated lipogenesis

A) 22 GO biological processes that were upregulated by glutamate and downregulated panEAAT inhibition (TFBTBOA) in RNAseq. -logPadj shown. N = 3 replicates/group.

B) Fasn mRNA expression as measured by real time qPCR after treatment with glutamate +/- panEAAT inhibition (TFBTBOA). **,****p<0.01, 0.0001 Sidak's multiple comparisons. Mean ± SEM of N = 3 replicates/experiment, 3 independent experiments.

C) EdU+ cell counts after treatment with glutamate +/- inhibitor of FASN (orlistat). Mean ± SEM of N = 4 replicates/experiment, 4 independent experiments. *p<0.05 Sidak's multiple comparisons.

D) Phosphor-mTOR/total mTOR in NSCs treated with glutamate +/- panEAAT inhibition (TFBTBOA). *,**p<0.05, 0.01 Tukey's multiple comparisons. Mean ± SEM of N = 2-3 replicates/experiment, 3 independent experiments.

E) EdU+ cell counts after treatment with glutamate +/- inhibitors of ryanodine receptor (αRYR, dantrolene) and glutamate dehydrogenase (αGDH, EGCG). *,**,***p<0.05, 0.01, 0.001 Sidak's multiple comparisons. Mean ± SEM of N = 4 replicates/experiment, 4 independent experiments.

Ca^{2+} release from the endoplasmic reticulum (ER) via the ER-bound ryanodine receptor (RyR)[36,37]. Blocking RyR alone with the inhibitor dantrolene (αRYR) did not significantly affect NSC proliferation (Fig 4E, S4G).

We next considered a role for glutamate as a substrate for metabolism. Conversion of glutamate to α-ketoglutarate directly fuels lipogenesis by contributing to TCA cycle generation of acetyl-CoA, which is a primary substrate for FASN-mediated de novo fatty acid synthesis. Inhibition of glutamate dehydrogenase (αGDH), the key enzyme for conversion of glutamate to α-ketoglutarate, had no effect on NSCs alone, but when combined with RyR inhibition, glutamate-induced proliferation was completely blocked (Fig 4E, S4G). These data suggest that release of ER Ca^{2+} and glutamate substrate metabolism jointly mediate glutamate transport-induced stimulation of NSC self-renewal (Fig S4H).

Discussion

Our findings suggest a functional, cell-autonomous role for EAAT1 in supporting adult hippocampal neurogenesis. Our findings stand in contrast to a canonical glutamate receptor-dependent mechanism for glutamate response reported in most other cell types and suggest that EAAT1 expressed by NSCs directly supports self-renewing proliferation via transport-dependent stimulation of lipogenesis.

Expression of glutamate transporter proteins, particularly EAAT1, is widespread in the radial glia NSCs of the embryonic forebrain[38]. One study in early postnatal DG NSCs concluded that EAATs indirectly suppress proliferation by limiting the activation of mGluRs[39]. This apparent reversal of the roles of EAAT1 and mGluR5 in early postnatal versus what we observed in adult DG NSCs is paralleled by downregulated expression of mGluR5 and upregulated expression of EAAT1 in DG NSCs during the transition to adulthood[40]. This transition could contribute to the shift in cellular behavior of DG NSCs from rapidly proliferating and depleting early in life to more maintenance-focused later in life[41]. Comparative studies of EAAT function in NSCs across different stages of development could shed further light on this hypothesis.

Our data support depolarization-sensitive RyR-mediated Ca^{2+} release as a process downstream of glutamate signaling that can mediate glutamate-induced NSC proliferation but only in combination with glutamate conversion to the TCA cycle substrate α-ketoglutarate. The putative need for glutamate as a metabolic substrate to stimulate NSC self-renewal provides a parsimonious explanation for why NSC depolarization secondary to glutamate receptor activation alone would not be as effective as glutamate itself in stimulating NSC proliferation[14].

Cell metabolic states are becoming increasingly recognized as active players in NSC self-renewal and fate decisions, both as generators of key cellular substrates for growth and as independent initiators of gene expression[42–44] . Several previous studies demonstrate a particularly critical role for fatty acid synthesis in DG NSC self-renewal[29–31]. In agreement with this previous data, we found that FASN activity was required for glutamate-induced NSC proliferation. Cell metabolism therefore represents a potential convergence point for the various glutamate-stimulated, EAAT-dependent processes that we observed in adult DG NSCs.

NSCs may derive glutamatergic input from multiple sources in vivo. NSC apical processes wrap around putatively glutamatergic synaptic terminals in the molecular layer of the DG[45]. Inputs here from hilar mossy cells[14] and hypothalamus[13] both stimulate NSC self-renewal, as does release from local astrocytes[12]. With multiple sources of glutamate, it is tempting to speculate

that changes in hippocampal glutamate signaling that occur during normal development, neurodegenerative pathology, and plasticity-inducing stimuli[46–49] could be transduced by EAAT1 into metabolic states that regulate the population maintenance of NSCs. Future studies could examine whether changes in EAAT expression or function modulate the response of NSCs to these physiological states.

In summary, we show that glutamate transport via EAAT1 cell-autonomously supports DG NSC self-renewal in adult mice. These findings help resolve some discrepancy in the field about the role of glutamate receptors versus glutamate itself in NSC maintenance. They also raise additional questions about the interplay between glutamate signaling and NSC behavior in contexts such as biological aging, neurological disorders, and plasticity-inducing stimuli like exercise and enriched environment[10,50,51].

Limitations of the study

The presented studies only examine NSCs in the adult DG of mice. The NSCs in the adult subventricular zone neurogenic niche also express EAAT1[52], and the role of EAAT1 in this niche remains an open question, to the best of our knowledge. Whether these results extend to other species, including primates, is also not yet clear either. However, a recent scRNAseq profiling of adult macaque hippocampal NSCs show high levels of EAAT1 and EAAT2 expression[53], suggesting the possibility that NSCs in adult primate hippocampus could rely on EAAT-mediated glutamate transport. We also do not resolve which glutamatergic inputs impact NSCs directly via EAAT1, nor how EAATs come in to play in pathological conditions characterized by excess glutamate transmission. Our work also only begins the uncovering of the intracellular signaling between glutamate transport and stimulation of FASN and NSC self-renewal. These steps will require more detailed investigation in the future.

Acknowledgements

This research was supported by R21 NS123797 from NINDS/NIH to EDK.

Research reported in this publication was supported by The Ohio State University Comprehensive Cancer Center and the National Institutes of Health under grant number P30 CA016058. We thank the Genomics Shared Resource at The Ohio State University Comprehensive Cancer Center, Columbus, OH for RNAseq services. We also thank the Cancer Program IT resource for sponsoring site licenses for GraphPad Prism and Biorender.

Author contributions

Conceptualization, JDR and EDK; Methodology, JDR and EDK; Investigation, JDR, IRB, JEC, EA, DE, AW, and VV; Writing – Original Draft, JDR and EDK; Writing – Reviewing and Editing, JDR and EDK; Supervision, JPB and EDK; Funding Acquisition, EDK.

Declaration of interests

V. Valentini is currently a consultant for Antec Scientific, USA, a role acquired in Oct 2019 after the completion of the relevant uHPLC-ECD studies but before the writing of the manuscript. The remaining authors declare no competing interests.

References

1. Borrett, M.J., Innes, B.T., Tahmasian, N., Bader, G.D., Kaplan, D.R., and Miller, F.D. (2022). A Shared Transcriptional Identity for Forebrain and Dentate Gyrus Neural Stem Cells from Embryogenesis to Adulthood. eNeuro *9*. 10.1523/ENEURO.0271-21.2021.

2. Götz, M., Nakafuku, M., and Petrik, D. (2016). Neurogenesis in the Developing and Adult Brain—Similarities and Key Differences. Cold Spring Harb Perspect Biol *8*, a018853. 10.1101/cshperspect.a018853.

3. Hochgerner, H., Zeisel, A., Lönnerberg, P., and Linnarsson, S. (2018). Conserved properties of dentate gyrus neurogenesis across postnatal development revealed by single-cell RNA sequencing. Nature Neuroscience *21*, 290–299. 10.1038/s41593-017-0056-2.

4. Hao, Z.-Z., Wei, J.-R., Xiao, D., Liu, R., Xu, N., Tang, L., Huang, M., Shen, Y., Xing, C., Huang, W., et al. (2022). Single-cell transcriptomics of adult macaque hippocampus reveals neural precursor cell populations. Nat Neurosci. 10.1038/s41593-022-01073-x.

5. Moreno-Jiménez, E.P., Flor-García, M., Terreros-Roncal, J., Rábano, A., Cafini, F., Pallas-Bazarra, N., Ávila, J., and Llorens-Martín, M. (2019). Adult hippocampal neurogenesis is abundant in neurologically healthy subjects and drops sharply in patients with Alzheimer's disease. Nature Medicine *25*, 554–560. 10.1038/s41591-019-0375-9.

6. Terreros-Roncal, J., Moreno-Jiménez, E.P., Flor-García, M., Rodríguez-Moreno, C.B., Trinchero, M.F., Cafini, F., Rábano, A., and Llorens-Martín, M. (2021). Impact of neurodegenerative diseases on human adult hippocampal neurogenesis. Science, eabl5163. 10.1126/science.abl5163.

7. Tobin, M.K., Musaraca, K., Disouky, A., Shetti, A., Bheri, A., Honer, W.G., Kim, N., Dawe, R.J., Bennett, D.A., Arfanakis, K., et al. (2019). Human Hippocampal Neurogenesis Persists in Aged Adults and Alzheimer's Disease Patients. Cell Stem Cell *24*, 974-982.e3. 10.1016/j.stem.2019.05.003.

8. Franjic, D., Skarica, M., Ma, S., Arellano, J.I., Tebbenkamp, A.T.N., Choi, J., Xu, C., Li, Q., Morozov, Y.M., Andrijevic, D., et al. (2021). Transcriptomic taxonomy and neurogenic trajectories of adult human, macaque, and pig hippocampal and entorhinal cells. Neuron, S0896627321008667. 10.1016/j.neuron.2021.10.036.

9. Sorrells, S.F., Paredes, M.F., Cebrian-Silla, A., Sandoval, K., Qi, D., Kelley, K.W., James, D., Mayer, S., Chang, J., Auguste, K.I., et al. (2018). Human hippocampal neurogenesis drops sharply in children to undetectable levels in adults. Nature *555*, 377–381. 10.1038/nature25975.

10. Berg, D.A., Belnoue, L., Song, H., and Simon, A. (2013). Neurotransmitter-mediated control of neurogenesis in the adult vertebrate brain. Development *140*, 2548–2561. 10.1242/dev.088005.

11. Toda, T., and Gage, F.H. (2018). Review: adult neurogenesis contributes to hippocampal plasticity. Cell Tissue Res *373*, 693–709. 10.1007/s00441-017-2735-4.

12. Asrican, B., Wooten, J., Li, Y.-D., Quintanilla, L., Zhang, F., Wander, C., Bao, H., Yeh, C.-Y., Luo, Y.-J., Olsen, R., et al. (2020). Neuropeptides Modulate Local Astrocytes to Regulate

Adult Hippocampal Neural Stem Cells. Neuron, S0896627320306048. 10.1016/j.neuron.2020.07.039.

13. Li, Y.-D., Luo, Y.-J., Chen, Z.-K., Quintanilla, L., Cherasse, Y., Zhang, L., Lazarus, M., Huang, Z.-L., and Song, J. (2022). Hypothalamic modulation of adult hippocampal neurogenesis in mice confers activity-dependent regulation of memory and anxiety-like behavior. Nat Neurosci *25*, 630–645. 10.1038/s41593-022-01065-x.

14. Yeh, C.-Y., Asrican, B., Moss, J., Quintanilla, L.J., He, T., Mao, X., Cassé, F., Gebara, E., Bao, H., Lu, W., et al. (2018). Mossy Cells Control Adult Neural Stem Cell Quiescence and Maintenance through a Dynamic Balance between Direct and Indirect Pathways. Neuron *99*, 493-510.e4. 10.1016/j.neuron.2018.07.010.

15. Cameron, H., McEwen, B., and Gould, E. (1995). Regulation of adult neurogenesis by excitatory input and NMDA receptor activation in the dentate gyrus. J. Neurosci. *15*, 4687–4692. 10.1523/JNEUROSCI.15-06-04687.1995.

16. Gould, E., McEwen, B.S., Tanapat, P., Galea, L.A.M., and Fuchs, E. (1997). Neurogenesis in the Dentate Gyrus of the Adult Tree Shrew Is Regulated by Psychosocial Stress and NMDA Receptor Activation. J. Neurosci. *17*, 2492–2498. 10.1523/JNEUROSCI.17-07-02492.1997.

17. Kitayama, T., Yoneyama, M., and Yoneda, Y. (2003). Possible regulation by N-methyl-d-aspartate receptors of proliferative progenitor cells expressed in adult mouse hippocampal dentate gyrus. Journal of Neurochemistry *84*, 767–780. 10.1046/j.1471-4159.2003.01567.x.

18. Nacher, J., Rosell, D.R., Alonso-Llosa, G., and McEwen, B.S. (2001). NMDA receptor antagonist treatment induces a long-lasting increase in the number of proliferating cells, PSA-NCAM-immunoreactive granule neurons and radial glia in the adult rat dentate gyrus. European Journal of Neuroscience *13*, 512–520. 10.1046/j.0953-816x.2000.01424.x.

19. DeCarolis, N.A., Mechanic, M., Petrik, D., Carlton, A., Ables, J.L., Malhotra, S., Bachoo, R., Götz, M., Lagace, D.C., and Eisch, A.J. (2013). In vivo contribution of nestin- and GLAST-lineage cells to adult hippocampal neurogenesis. Hippocampus *23*, 708–719. 10.1002/hipo.22130.

20. Yuzwa, S.A., Borrett, M.J., Innes, B.T., Voronova, A., Ketela, T., Kaplan, D.R., Bader, G.D., and Miller, F.D. (2017). Developmental Emergence of Adult Neural Stem Cells as Revealed by Single-Cell Transcriptional Profiling. Cell Reports *21*, 3970–3986. 10.1016/j.celrep.2017.12.017.

21. Regan, M.R., Huang, Y.H., Kim, Y.S., Dykes-Hoberg, M.I., Jin, L., Watkins, A.M., Bergles, D.E., and Rothstein, J.D. (2007). Variations in Promoter Activity Reveal a Differential Expression and Physiology of Glutamate Transporters by Glia in the Developing and Mature CNS. Journal of Neuroscience *27*, 6607–6619. 10.1523/JNEUROSCI.0790-07.2007.

22. Renzel, R., Sadek, A.-R., Chang, C.-H., Gray, W.P., Seifert, G., and Steinhäuser, C. (2013). Polarized distribution of AMPA, but not GABAA, receptors in radial glia-like cells of the adult dentate gyrus. Glia *61*, 1146–1154. 10.1002/glia.22505.

23. Wang, L.-P., Kempermann, G., and Kettenmann, H. (2005). A subpopulation of precursor cells in the mouse dentate gyrus receives synaptic GABAergic input. Molecular and Cellular Neuroscience *29*, 181–189. 10.1016/j.mcn.2005.02.002.

24. Shin, J., Berg, D.A., Zhu, Y., Shin, J.Y., Song, J., Bonaguidi, M.A., Enikolopov, G., Nauen, D.W., Christian, K.M., Ming, G., et al. (2015). Single-Cell RNA-Seq with Waterfall Reveals Molecular Cascades underlying Adult Neurogenesis. Cell Stem Cell *17*, 360–372. 10.1016/j.stem.2015.07.013.

25. Mignone, J.L., Kukekov, V., Chiang, A.-S., Steindler, D., and Enikolopov, G. (2004). Neural stem and progenitor cells in nestin-GFP transgenic mice. Journal of Comparative Neurology *469*, 311–324. 10.1002/cne.10964.

26. Babu, H., Claasen, J.-H., Kannan, S., Rünker, A.E., Palmer, T., and Kempermann, G. (2011). A Protocol for Isolation and Enriched Monolayer Cultivation of Neural Precursor Cells from Mouse Dentate Gyrus. Front. Neurosci. *5*. 10.3389/fnins.2011.00089.

27. Denninger, J.K., Chen, X., Turkoglu, A.M., Sarchet, P., Volk, A.R., Rieskamp, J.D., Yan, P., and Kirby, E.D. (2020). Defining the adult hippocampal neural stem cell secretome: In vivo versus in vitro transcriptomic differences and their correlation to secreted protein levels. Brain Research *1735*, 146717. 10.1016/j.brainres.2020.146717.

28. Thakore, P.I., D'Ippolito, A.M., Song, L., Safi, A., Shivakumar, N.K., Kabadi, A.M., Reddy, T.E., Crawford, G.E., and Gersbach, C.A. (2015). Highly specific epigenome editing by CRISPR-Cas9 repressors for silencing of distal regulatory elements. Nature Methods *12*, 1143–1149. 10.1038/nmeth.3630.

29. Knobloch, M., Pilz, G.-A., Ghesquière, B., Kovacs, W.J., Wegleiter, T., Moore, D.L., Hruzova, M., Zamboni, N., Carmeliet, P., and Jessberger, S. (2017). A Fatty Acid Oxidation-Dependent Metabolic Shift Regulates Adult Neural Stem Cell Activity. Cell Reports *20*, 2144–2155. 10.1016/j.celrep.2017.08.029.

30. Knobloch, M., Braun, S.M.G., Zurkirchen, L., von Schoultz, C., Zamboni, N., Araúzo-Bravo, M.J., Kovacs, W.J., Karalay, Ö., Suter, U., Machado, R.A.C., et al. (2013). Metabolic control of adult neural stem cell activity by Fasn-dependent lipogenesis. Nature *493*, 226–230. 10.1038/nature11689.

31. Ramosaj, M., Madsen, S., Maillard, V., Scandella, V., Sudria-Lopez, D., Yuizumi, N., Telley, L., and Knobloch, M. (2021). Lipid droplet availability affects neural stem/progenitor cell metabolism and proliferation. Nat Commun *12*, 7362. 10.1038/s41467-021-27365-7.

32. López-Colomé, A.M., Martínez-Lozada, Z., Guillem, A.M., López, E., and Ortega, A. (2012). Glutamate Transporter-Dependent mTOR Phosphorylation in Müller Glia Cells. ASN Neuro *4*, AN20120022. 10.1042/AN20120022.

33. Martínez-Lozada, Z., Hernández-Kelly, L.C., Aguilera, J., López-Bayghen, E., and Ortega, A. (2011). Signaling through EAAT-1/GLAST in cultured Bergmann glia cells. Neurochemistry International *59*, 871–879. 10.1016/j.neuint.2011.07.015.

34. Cavallucci, V., Fidaleo, M., and Pani, G. (2016). Neural Stem Cells and Nutrients: Poised Between Quiescence and Exhaustion. Trends in Endocrinology & Metabolism *27*, 756–769. 10.1016/j.tem.2016.06.007.

35. Zhu, J., and Thompson, C.B. (2019). Metabolic regulation of cell growth and proliferation. Nat Rev Mol Cell Biol *20*, 436–450. 10.1038/s41580-019-0123-5.

36. Lobos, P., Córdova, A., Vega-Vásquez, I., Ramírez, O.A., Adasme, T., Toledo, J., Cerda, M., Härtel, S., Paula-Lima, A., and Hidalgo, C. (2021). RyR-mediated Ca2+ release elicited by neuronal activity induces nuclear Ca2+ signals, CREB phosphorylation, and Npas4/RyR2 expression. Proceedings of the National Academy of Sciences *118*, e2102265118. 10.1073/pnas.2102265118.

37. Ouardouz, M., Nikolaeva, M.A., Coderre, E., Zamponi, G.W., McRory, J.E., Trapp, B.D., Yin, X., Wang, W., Woulfe, J., and Stys, P.K. (2003). Depolarization-Induced Ca2+ Release in Ischemic Spinal Cord White Matter Involves L-type Ca2+ Channel Activation of Ryanodine Receptors. Neuron *40*, 53–63. 10.1016/j.neuron.2003.08.016.

38. Anthony, T.E., Klein, C., Fishell, G., and Heintz, N. (2004). Radial Glia Serve as Neuronal Progenitors in All Regions of the Central Nervous System. Neuron *41*, 881–890. 10.1016/S0896-6273(04)00140-0.

39. Gilley, J.A., and Kernie, S.G. (2011). Gltl and Glast negatively regulate calcium-dependent proliferation of hippocampal neural progenitor cells and are persistently upregulated after injury. Eur J Neurosci *34*, 1712–1723. 10.1111/j.1460-9568.2011.07888.x.

40. Berg, D.A., Su, Y., Jimenez-Cyrus, D., Patel, A., Huang, N., Morizet, D., Lee, S., Shah, R., Ringeling, F.R., Jain, R., et al. (2019). A Common Embryonic Origin of Stem Cells Drives Developmental and Adult Neurogenesis. Cell *177*, 654-668.e15. 10.1016/j.cell.2019.02.010.

41. Harris, L., Rigo, P., Stiehl, T., Gaber, Z.B., Austin, S.H.L., Masdeu, M. del M., Edwards, A., Urbán, N., Marciniak-Czochra, A., and Guillemot, F. (2021). Coordinated changes in cellular behavior ensure the lifelong maintenance of the hippocampal stem cell population. Cell Stem Cell *0*. 10.1016/j.stem.2021.01.003.

42. Madsen, S., Ramosaj, M., and Knobloch, M. (2021). Lipid metabolism in focus: how the build-up and breakdown of lipids affects stem cells. Development *148*, dev191924. 10.1242/dev.191924.

43. Wani, G.A., Sprenger, H.-G., Ndoci, K., Chandragiri, S., Acton, R.J., Schatton, D., Kochan, S.M.V., Sakthivelu, V., Jevtic, M., Seeger, J.M., et al. (2022). Metabolic control of adult neural stem cell self-renewal by the mitochondrial protease YME1L. Cell Reports *38*. 10.1016/j.celrep.2022.110370.

44. Kandel, P., Semerci, F., Mishra, R., Choi, W., Bajic, A., Baluya, D., Ma, L., Chen, K., Cao, A.C., Phongmekhin, T., et al. (2022). Oleic acid is an endogenous ligand of TLX/NR2E1 that triggers hippocampal neurogenesis. Proceedings of the National Academy of Sciences *119*, e2023784119. 10.1073/pnas.2023784119.

45. Moss, J., Gebara, E., Bushong, E.A., Sánchez-Pascual, I., O'Laoi, R., M'Ghari, I.E., Kocher-Braissant, J., Ellisman, M.H., and Toni, N. (2016). Fine processes of Nestin-GFP–positive

radial glia-like stem cells in the adult dentate gyrus ensheathe local synapses and vasculature. PNAS *113*, E2536–E2545. 10.1073/pnas.1514652113.

46. Hascup, K.N., Findley, C.A., Sime, L.N., and Hascup, E.R. (2020). Hippocampal alterations in glutamatergic signaling during amyloid progression in AβPP/PS1 mice. Sci Rep *10*, 14503. 10.1038/s41598-020-71587-6.

47. Segovia, G., Yagüe, A.G., García-Verdugo, J.M., and Mora, F. (2006). Environmental enrichment promotes neurogenesis and changes the extracellular concentrations of glutamate and GABA in the hippocampus of aged rats. Brain Research Bulletin *70*, 8–14. 10.1016/j.brainresbull.2005.11.005.

48. Świątkiewicz, M., Fiedorowicz, M., Orzeł, J., Wełniak-Kamińska, M., Bogorodzki, P., Langfort, J., and Grieb, P. (2017). Increases in Brain 1H-MR Glutamine and Glutamate Signals Following Acute Exhaustive Endurance Exercise in the Rat. Frontiers in Physiology *8*.

49. Vivar, C., and van Praag, H. (2017). Running Changes the Brain: the Long and the Short of It. Physiology *32*, 410–424. 10.1152/physiol.00017.2017.

50. Wander, C.M., and Song, J. (2021). The neurogenic niche in Alzheimer's disease. Neuroscience Letters *762*, 136109. 10.1016/j.neulet.2021.136109.

51. Rodríguez-Bodero, A., and Encinas-Pérez, J.M. (2022). Does the plasticity of neural stem cells and neurogenesis make them biosensors of disease and damage? Frontiers in Neuroscience *16*.

52. Fuentealba, L.C., Obernier, K., and Alvarez-Buylla, A. (2012). Adult Neural Stem Cells Bridge Their Niche. Cell Stem Cell *10*, 698–708. 10.1016/j.stem.2012.05.012.

53. Wang, W., Wang, M., Yang, M., Zeng, B., Qiu, W., Ma, Q., Jing, X., Zhang, Q., Wang, B., Yin, C., et al. (2022). Transcriptome dynamics of hippocampal neurogenesis in macaques across the lifespan and aged humans. Cell Res *32*, 729–743. 10.1038/s41422-022-00678-y.

Supplementary Figures

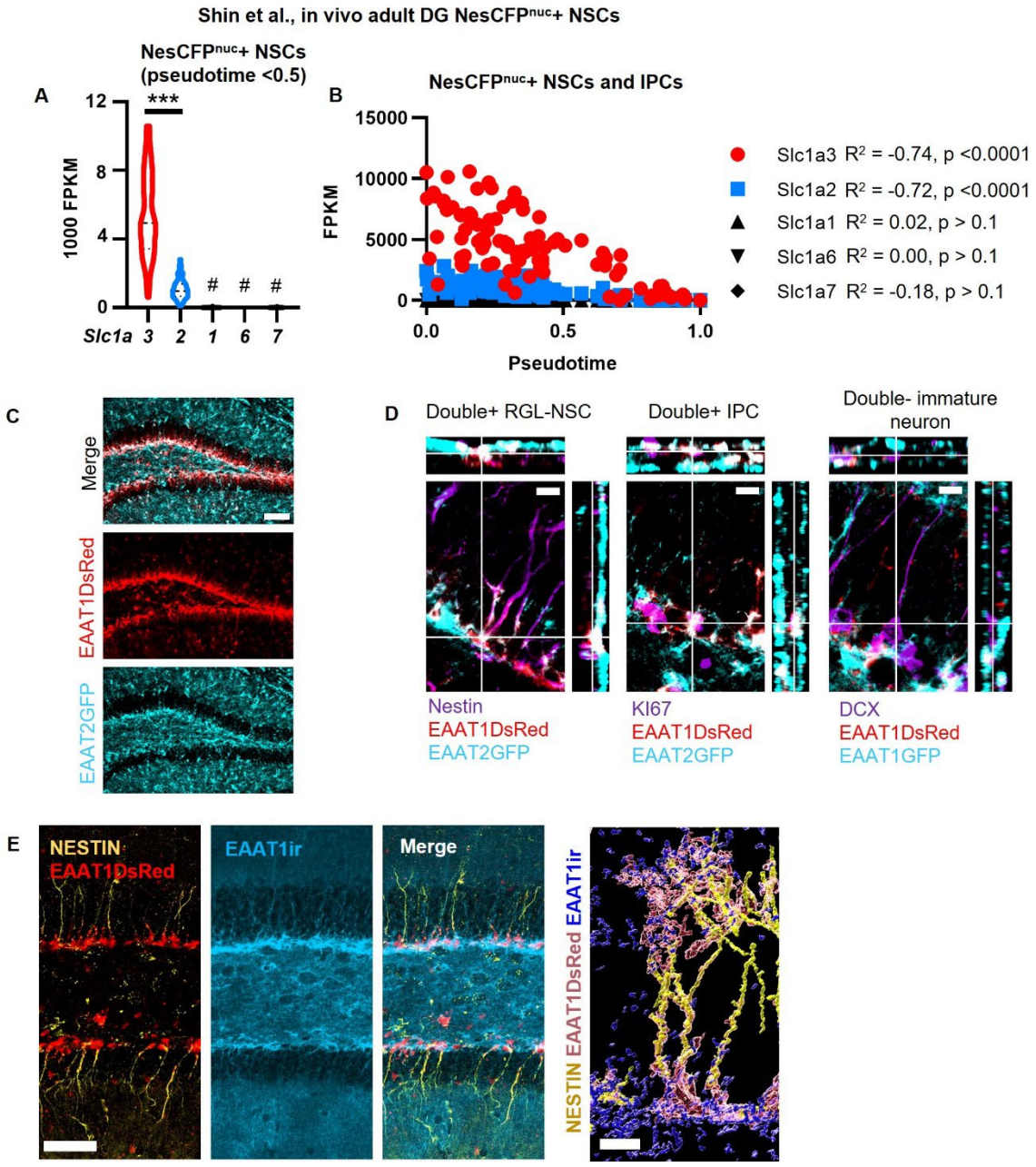

Sup Fig 1: Supplement to Fig 1

A) scRNAseq FPKM values for EAAT transcripts from data in Shin et al., 2015. Only cells with psuedotime <0.5 included to reflect NSCs (as opposed to early IPCs). ***p<0.001, #p<0.0001 vs EAAT1 and 2, Dunn's multiple comparisons

B) FPKM of EAAT1-5 by pseudotime from Shin et al., 2015. Pearson R^2 values.

C) EAAT1DsRed+EAAT2GFP+ fluorescence in the adult DG. Scale = 100 µm.

D) Orthogonal projections of example: EAAT1DsRed+EAAT2GFP+ (double+) Nestin+ radial glia like (RGL) NSC, EAAT1DsRed+EAAT2GFP+ (double+) Ki67+ IPC, EAAT1DsRed-EAAT2GFP- (double-) DCX+ immature neuron. Scale = 10 µm.

E) Nestin immunolabeling in DG of EAAT1DsRed+ co-localized with EAAT1 immunoreactivity (ir). Left is merged z-stack. Right is 3D reconstruction showing an example Nestin+EAAT1DsRed+ radial glia like NSC with EAAT1ir in the cell body and apical terminals.

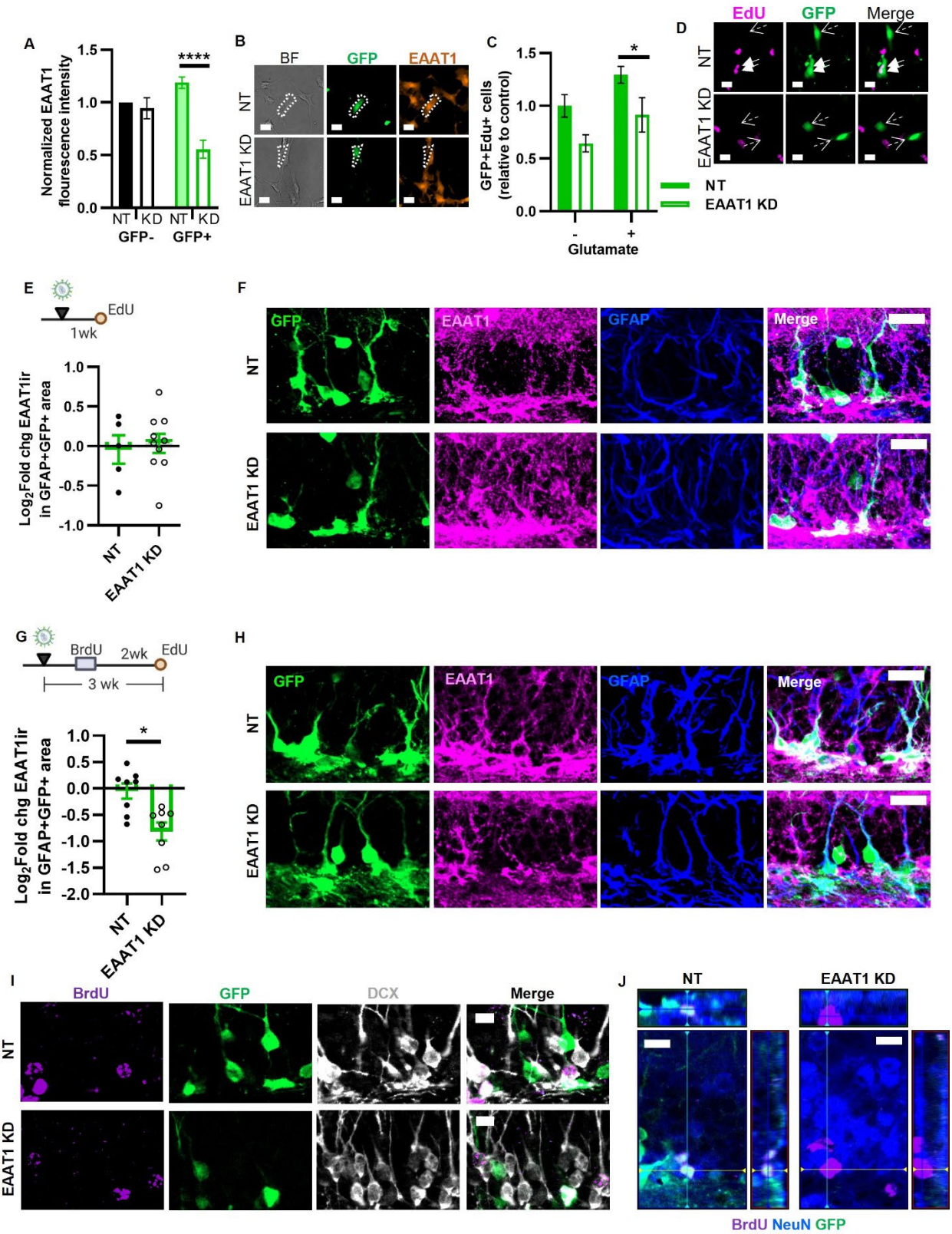

Sup Fig 2: Supplement to Fig 2

A) FPKM of glutamate receptor genes from Shin et al., 2015 with EAAT1 and EAAT2 included for scale.

B) Transcript length-normalized RNAseq counts of glutamate receptor genes and EAAT1/2 from cultured adult DG NSCs in Denninger et al., 2020.
C) emPAI length-normalized semi-quantitiative spectral counts for glutamate receptor and transporter proteins from cultured adult DG NSCs in Denninger et al., 2020.
D) Representative image of EdU+ labeling in cultured NSCs after L-aspartate treatment +/- NMDA receptor inhibitor (AP5), with Hoechst to label nuclei. Scale = 20 µm.
E) Representative image of EdU+ labeling in cultured NSCs after glutamate receptor agonist tretament, with Hoechst to label nuclei. Scale = 20 µm.
F) Glutamate in conditioned media as measured by uHPLC after a 5 µM pulse in wells with NSCs or empty wells. ***,****$p<0.001$, 0.0001 vs “No Cells” Sidak’s multiple comparisons. Mean ± SEM of N = 6 independent experiments.
G) Glutamate in NSC conditioned media as measured by uHPLC after a 5 µM pulse after pre-treatment with an EAAT2-selective (1 µM) and an EAAT1and2 selective (10 µM) dose of WAY213613. *$p<0.05$ vs 1 µM and vs 10 µM. Mean ± SEM of N = 6 independent experiments.
H) Glutamate in NSC conditioned media as measured by uHPLC after a 5 µM pulse after pre-treatment with a panEAAT inhibitor (TFB-TBOA), an EAAT1 inhibitor (UCPH101), or and EAAT2 inhibitor (DHK). *$p<0.05$ Tukey’s comparisons within timepoint. Mean ± SEM of N = 3 independent experiments.
I) Representative image of EdU+ labeling in cultured NSCs after treatment with EAAT inhibitors, with Hoechst to label nuclei. Scale = 20 µm.
J) Sapphire IR signal in cultured NSCs after treatment with glutamate +/- panEAAT inhibitor (TFB-TBOA) or EAAT1 inhibitor (UCPH101). Protein transport inhibitor at toxic dose is positive control for presence of apoptosis in Sapphire IR700 assay. ****$p<0.0001$ Dunnett’s multiple comparisons each group vs positive control. Mean ± SEM of N = 3-6 replicates/experiment, 2 independent experiments. Top shows representative image of Sapphire IR signal in treatment groups.

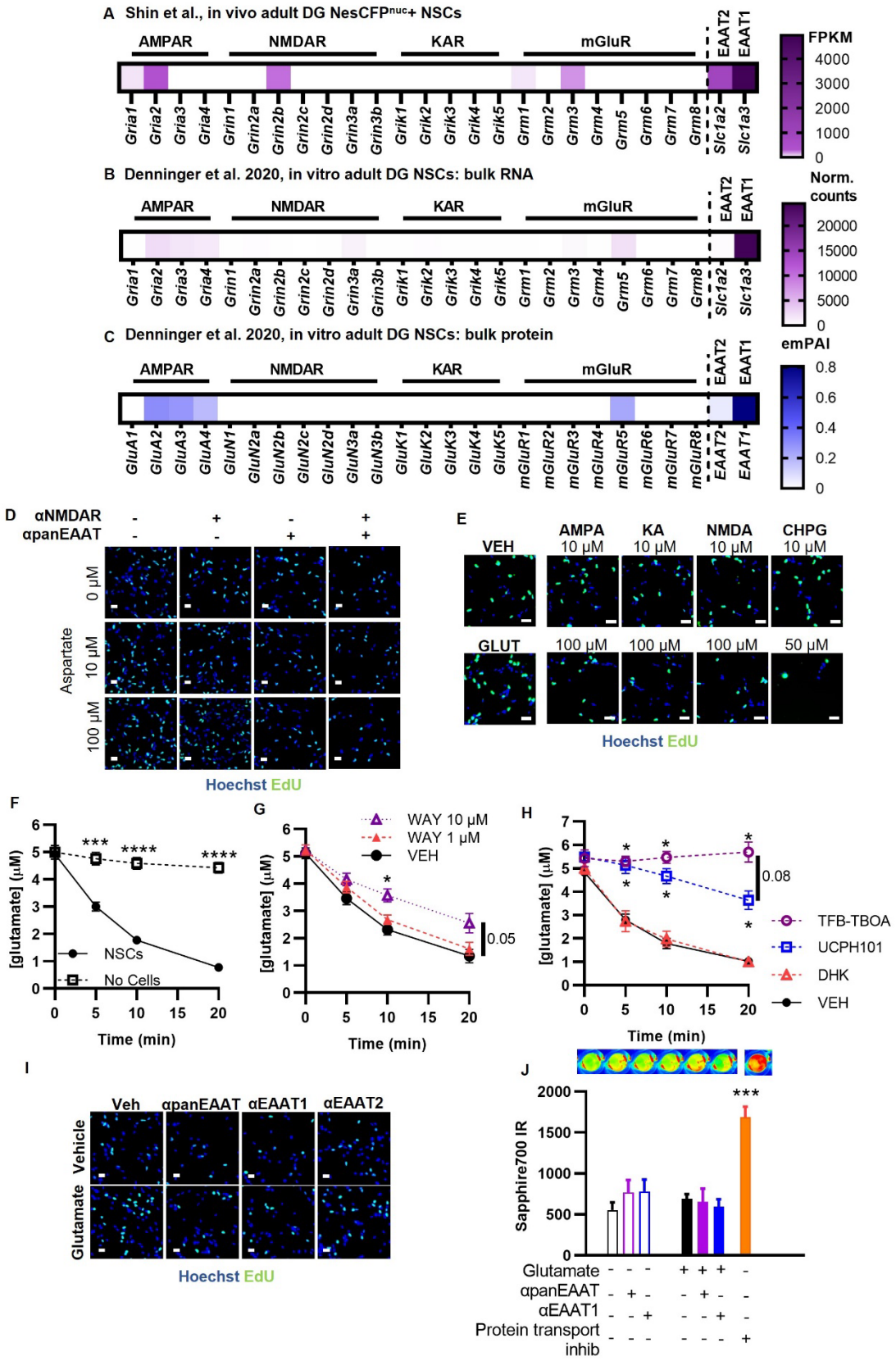
A Shin et al., in vivo adult DG NesCFP^nuc+ NSCs
AMPAR
NMDAR
KAR
mGluR
EAAT2
EAAT1
FPKM
4000
3000
2000
1000
0
Gria1 Gria2 Gria3 Gria4 Grin1 Grin2a Grin2b Grin2c Grin2d Grin3a Grin3b Grik1 Grik2 Grik3 Grik4 Grik5 Grm1 Grm2 Grm3 Grm4 Grm5 Grm6 Grm7 Grm8 Slc1a2 Slc1a3
B Denninger et al. 2020, in vitro adult DG NSCs: bulk RNA
Norm. counts
20000
15000
10000
5000
0
C Denninger et al. 2020, in vitro adult DG NSCs: bulk protein
emPAI
0.8
0.6
0.4
0.2
0
GluA1 GluA2 GluA3 GluA4 GluN1 GluN2a GluN2b GluN2c GluN2d GluN3a GluN3b GluK1 GluK2 GluK3 GluK4 GluK5 mGluR1 mGluR2 mGluR3 mGluR4 mGluR5 mGluR6 mGluR7 mGluR8 EAAT2 EAAT1
D αNMDAR - + - +
αpanEAAT - - + +
Aspartate
0 μM
10 μM
100 μM
Hoechst EdU
E
VEH
AMPA 10 μM
KA 10 μM
NMDA 10 μM
CHPG 10 μM
GLUT
100 μM
100 μM
100 μM
50 μM
Hoechst EdU
F
[glutamate] (μM)
Time (min)
NSCs
No Cells
***
****
****
G
WAY 10 μM
WAY 1 μM
VEH
0.05
H
0.08
TFB-TBOA
UCPH101
DHK
VEH
I
Veh
αpanEAAT
αEAAT1
αEAAT2
Vehicle
Glutamate
Hoechst EdU
J
Sapphire700 IR
2000
1500
1000
500
0
***
Glutamate
αpanEAAT
αEAAT1
Protein transport inhib

Sup Fig 3: Supplement to Fig 3

A) EAAT1 immunoreactive intensity in cultured NSCs infected with NT and EAAT1 KD CRISPRi lentiviral vectors. ****p<0.0001 Sidak's multiple comparisons within GFP type. Mean ± SEM of N = 4 independent infections.
B) Representative images of EAAT1 labeling coupled with GFP and brightfield to visualize all NSCs. Scale = 10 µm.
C) EdU+GFP+ cell counts in cultured NSCs infected with NT and EAAT1 KD CRISPRi lentiviral vectors. Mean ± SEM of N = 3 replicates/infection, 3 independent infections.
D) Representative images of EdU labeling coupled with GFP in NSCs infected with NT and EAAT1 KD CRISPRi lentiviral vectors. Scale = 10 µm.
E) Timeline and EAAT1 immunolabeling intensity within GFP+GFAP+ area of mice infused with NT or EAAT1 KD CRISPRi lentiviral vectors in the DG then perfused 1 week later. Mean ± SEM of N = 5-8 individual mice (points shown).
F) Representative image of EAAT1 labeling coupled with GFP and GFAP at 1 week after CRISPRi infusion. Co-labeling becomes white in merged image. Scale = 20 µm.
G) Timeline and EAAT1 immunolabeling intensity within GFP+GFAP+ area of mice infused with NT or EAAT1 KD CRISPRi lentiviral vectors in the DG then perfused 3 weeks later. *p<0.05 Mann Whitney test. Mean ± SEM of N = 8 individual mice (points shown).
H) Representative image of EAAT1 labeling coupled with GFP and GFAP at 3 weeks after CRISPRi infusion. Co-labeling becomes white in merged image. Scale = 20 µm.
I) Representative image of BrdU, GFP, DCX co-labeling 3 weeks after CRISPRi vector infusion. Scale = 10 µm.
J) Representative orthogonal view of a BrdU+NeuN+GFP+ cell in a NT infused mouse and a BrdU+NeuN+GFP- cell in an EAAT1 KD infused mouse. Scale = 10 µm.

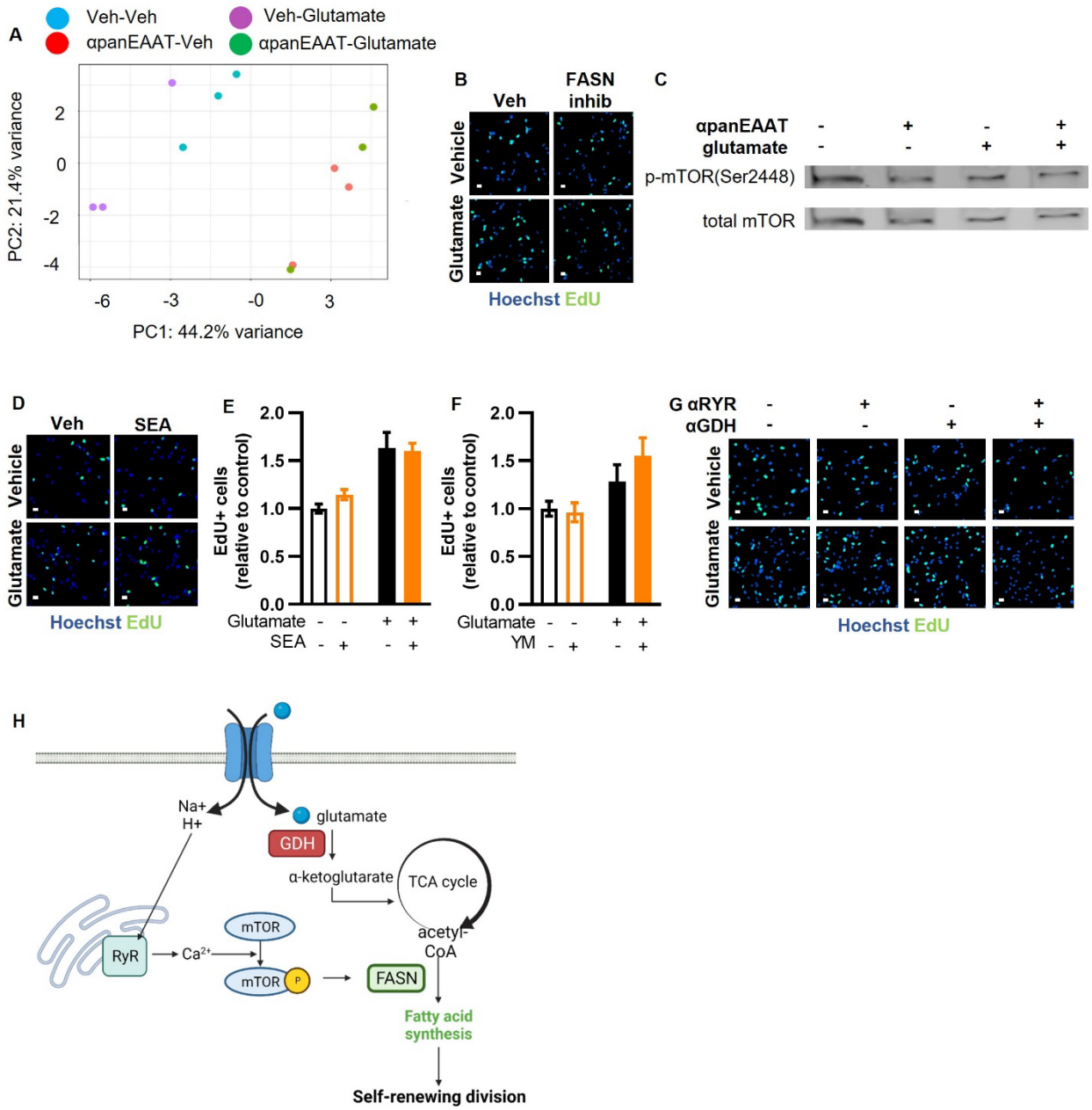

Sup Fig 4: Supplement to Figure 4

A) Principle component analysis of RNAseq samples from treated in vitro NSCs.
B) Representative images of EdU labeling in NSCs treated with glutamate +/- FASN inhibitor orlistat. Hoechst as nuclear marker. Scale = 10 µm.
C) Representative blot of phosphor-mTOR and total mTOR in NSCs glutamate +/- panEAAT inhibitor (TFB-TBOA).
D) Representative images of EdU labeling in NSCs treated with glutamate +/- NCX inhibitor SEA0400. Hoechst as nuclear marker. Scale = 10 µm.
E) EdU+ cell counts after treatment with glutamate +/- NCX inhibitor SEA0400. Mean ± SEM of N = 4 replicates/experiment, 4 independent experiments.
F) EdU+ cell counts after treatment with glutamate +/- NCX inhibitor YM244769. *,**,***p<0.05, 0.01, 0.001 Sidak's multiple comparisons. Mean ± SEM of N = 2 replicates/experiment, 4 independent experiments.
G) Representative images of EdU labeling in NSCs treated with glutamate +/- NCX inhibitor YM244769. Hoechst as nuclear marker. Scale = 10 µm.
H) Model of proposed glutamate transport intracellular signaling.